



CYGNSS 海表风场观测数据验证及其可能的应用

摘要

海表面风场可以用于获取许多大气和海洋现象的信号,高质量、高时空分辨率的海表面风场数据产品将有利于海洋-大气动力过程的研究.本文使用全球热带系泊浮标阵列计划(Global Tropical Moored Array Programs)的锚定浮标风场数据和西沙通量塔气象观测资料验证了Cyclone Global Navigation Satellite System(CYGNSS)的35°N~35°S海面遥感风场观测数据.结果表明,CYGNSS海表面风场与实测资料存在着2.17 m/s左右的平均均方根误差(RMSD),它可能源于观测数据和卫星遥感资料的观测误差,以及两者在空间和时间上未严格匹配而引起的代表性误差.另外,CYGNSS海表面风速的时间演变与实测资料非常一致,展现了CYGNSS在研究海洋-大气能量和动量交换过程方面的潜在应用价值.本文使用Madden-Julian Oscillation(MJO)和赤道东部印度洋上升流事件作为两个个例,说明了CYGNSS海表面风场资料的潜在应用价值.

关键词

CYGNSS; 观测数据; 验证; 潜在应用; MJO; 沿岸上升流

中图分类号 P414.4

文献标志码 A

收稿日期 2018-04-10

资助项目 中国科学院战略性先导科技专项(XDA2006050301)

作者简介

胡运,男,博士生,研究方向为MJO影响下的海气相互作用. huyunhappy@foxmail.com

1 南京信息工程大学 大气科学学院,南京,210044

2 南京信息工程大学 海洋科学学院,南京,210044

3 中国科学院南海海洋研究所,广州,510301

0 导读

本文原文为英文,希望感兴趣的读者进一步关注原文.

海表风场是海气界面主要的动量通量和能量通量的来源.为了正确认识海气相互作用过程,需要进一步提高海表风场数据的质量、时间和空间分辨率,以便模拟和预测海洋和大气现象的发生及发展过程.现有的海表风场数据的时间和空间分辨率逐渐提高,但降水对风场数据的影响仍然存在.2016年底,美国航空航天局的旋风全球导航卫星系统(CYGNSS)飞行任务启动,它是一个用于提高飓风预报准确性的包含8颗微小卫星的星座,可以对热带气旋、台风以及飓风整个寿命周期中的眼壁内和眼壁附近的海洋表面风进行频繁测量,每秒可得到32个实际风速值.另外,CYGNSS观测系统可对单一样本点进行多次观测,时间间隔为几分钟至几小时.总之,CYGNSS观测数据具有两个明显优点:1)几乎不受降水影响;2)时间步长短.

本文使用较多的单点观测数据来验证CYGNSS观测数据的可靠性.选取的时间段为2017年8月1日—10月4日,共65 d.首先将CYGNSS风场数据与中国南海西沙通量塔风场数据进行对比.卫星数据与站点观测存在着2.49 m/s的均方根误差(RMSD).另外,时间上均匀、空间上网格化的CYGNSS风场产品更适用于海洋和大气的研究.将CYGNSS风场数据与全球热带系泊浮标阵列计划的锚定浮标风场数据进行对比,结果显示,相对于锚定浮标数据,CYGNSS风场产品存在着2.17 m/s的平均RMSD.该数值符合CYGNSS任务数据产品的要求,即低于20 m/s风速时,其反演不确定性为2.0 m/s.这些误差可能源于观测数据和卫星资料的观测误差,以及两者在空间和时间上未严格匹配而引起的代表性误差.CYGNSS海表面风速的时间演变与实测资料非常一致,展现了CYGNSS在研究海洋-大气能量和动量交换过程方面的潜在应用价值.

为了展现CYGNSS数据产品的潜在应用价值,本文使用Madden-Julian Oscillation(MJO)和赤道东部印度洋上升流事件作为两个个例,验证CYGNSS风场在获取两者信号时的表现.结果表明,CYGNSS海表风场较好地展现了MJO东传的速度和位相,这与850 hPa风场表现一致;同时,CYGNSS海表风场可通过算法来指示赤道印度洋东部上升流的强度,该强度与海表温度异常值变化一致.

Validation of CYGNSS observation and its potential applications

HU Yun¹ WANG Xiaochun² WANG Dongxiao³

1 School of Atmospheric Sciences, Nanjing University of Information Science & Technology, Nanjing 210044

2 School of Marine Sciences, Nanjing University of Information Science & Technology, Nanjing 210044

3 South China Sea Institute of Oceanology, Chinese Academy of Sciences, Guangzhou 510301

Abstract Many phenomena in the atmosphere and the ocean can be detected by sea surface winds. High quality and high temporal and spatial resolution sea surface wind data product is needed to study these phenomena. In this paper, sea surface winds from Cyclone Global Navigation Satellite System (CYGNSS) mission over 35°N–35°S are validated against in situ observations in order to evaluate the performance of CYGNSS. The in situ wind observations include measurements from the Xisha flux tower in South China Sea (SCS), and moored buoy data from the Global Tropical Moored Buoy Array (GT MBA). The result indicates a mean root-mean-square-difference (RMSD) of 2.17 m/s of CYGNSS winds with respect to in situ observations. Part of this discrepancy may come from instrument error, and part of it may come from representative error because of not-exact match of in situ and satellite measurements. The time evolution of CYGNSS winds, however, is consistent with that of in-situ winds, suggesting its potential application in understanding the complex mass and energy interchange processes of atmosphere and ocean. Examples using surface wind to analyze the MJO and the equatorial eastern Indian Ocean upwelling events are also discussed, which indicates potential applications of CYGNSS observation.

Key words CYGNSS; observations; validation; potential application; Madden-Julian oscillation; coastal upwelling

1 Introduction

Sea surface wind is the typical movement of near-surface air and the largest source of momentum for the upper ocean. It can drive ocean currents, develop convection via surface wind convergence and divergence^[1], and transfer heat flux, moisture, gases and particulates into and out of the ocean^[2]. Accurate measurements of sea surface wind will provide researchers with more detailed information about these dynamic processes of the atmosphere and the ocean. Throughout history, the poor spatial and temporal coverage of ship- and buoy-based observations set limits to describe meteorological conditions over the open ocean^[3]. Of late, as technology developed, many satellite-based monitoring methods have measured higher-quality wind datasets over tropical and global oceans^[4]. For instance, Quick Scatterometer provides global winds from 1999 to 2009^[5], and the National Centers for Environmental Prediction is involved to present two global reanalysis projects, including Reanalysis-1 and Reanalysis-2^[6-7]. The Cross-Calibrated Multi-Platform (CCMP) gridded surface vector winds are also widely used^[8]. Many

efforts have been made to evaluate or compare the existing wind data products. The resolution of measurements is improved due to the development of technology, while the rainfall effects on the quality of wind data is still a key limitation^[9-10].

At the end of 2016, the orbital injection of a single launch vehicle carrying a constellation of eight small satellites marks the beginning of the Cyclone Global Navigation Satellite System (CYGNSS) mission. One of the primary CYGNSS objectives is to leverage Global Positioning System (GPS) reflectometry to measure wind speeds in tropical cyclones (TCS) inner core with sufficient frequency to resolve genesis and rapid intensification phases of the TC life cycle^[11]. And another objective is to measure sea wind speeds under rainy conditions, especially those in the eye of the storm. Rather than previous satellite scatterometers, CYGNSS provides more samples of the study area. For instance, if compared with two current scatterometers combined, the percentage of 3-hour intervals that TC inner core regions can be sampled by satellite sensors is improved from 25% to nearly 35%.

Ground tracks for 6 hours in a particular day are

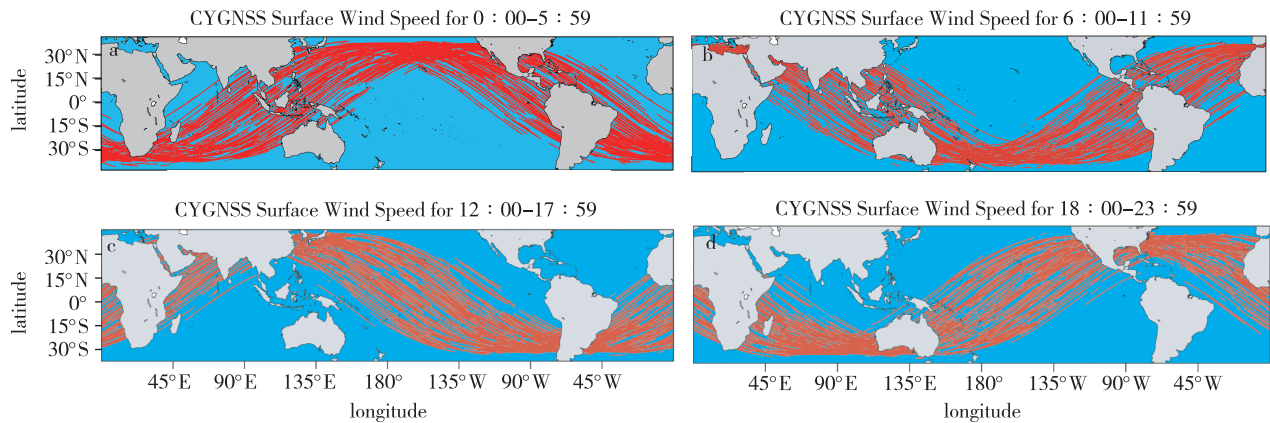


Fig. 1 Coverage of winds available from CYGNSS mission during different 6 hourly assimilation cycles on a particular days (a) from 0:00 to 5:59, (b) from 6:00 to 11:59, (c) from 12:00 to 17:59, (d) from 18:00 to 23:59

shown in Figure 1. Eight low earth orbit satellites with an inclination of 35 degrees to the equator are each capable of measuring 4 simultaneous reflections, resulting in 32 wind measurements per second across the globe^[12]. Besides, the satellite revisit time for the same geographical point during the science mission is reduced to a shorter time, few minutes to few hours. The median value of revisit times is 2.8 hours and the mean revisit time is 7.2 hours. Thus, these satellites provide space-based measurements with the following temporal and spatial sampling: (a) temporal sampling better than 12-hour mean revisit time and (b) spatial sampling 70% of all storm tracks between 35° N and 35° S latitude to be sampled within 24 hours. The number of satellites, their orbit altitudes and inclinations, and the alignment of the antennas are all optimized to provide unprecedented high temporal-resolution wind field imagery of TC genesis, intensification and decay.

Despite the focus on tropical cyclones, the ability of CYGNSS to provide rapid updates of winds, unbiased by the presence of rainfall, shows many other potential applications related to general tropical convection. A reliable application of near-surface wind conditions, observed at a given time at sea, is necessary for practically every kind of human activity both at open sea and in the coastal zone. The Madden-Julian oscillation (MJO) is a large-scale air-sea coupled process that propagates eastward at about 5 m/s with a period of 30–60 day, and the primary mode of intraseasonal variability in the tropical atmosphere^[13]. Strong MJO activity has significant

features with deep clouds, heavier rainfall and westerly wind anomalies. More information about MJO structure and the skill of MJO forecast require detailed knowledge of sea surface winds, which is limited by existing measurement systems and heavy rainfall due to the MJO^[12]. In addition, much of the signals of enhanced deep convective system comes from the result of empirical orthogonal functions of meteorological measurements, including outgoing long-wave radiation, 850 hPa and 250 hPa wind fields, or their combinations^[14]. Since the low-level zonal wind anomalies are out of phase with those at upper levels due to the MJO^[15], sea surface winds may be an alternative indicator for detecting the MJO signal. However, the greatest mean and diurnal maximum of rainfall rate over ocean exist in the MJO envelope. And in theory, little to no rainfall effect on CYGNSS measurements enables researchers to better understand the mechanisms of tropical deep convective system.

Besides the above, a more robust wind product is also needed by the research of ocean process. In the equatorial eastern Indian Ocean, surface water is driven by the strong, local southeast monsoon winds from June to October. Surface Ekman transport replaces the offshore moving water by upwelled water, leading to lower sea-level altitudes and cold sea surface temperature (SST) anomalies^[16]. However, long-time series of ocean surface currents are not available, and directly quantifying upwelling is also extremely difficult^[17]. The idea behind the offshore component of sur-

face Ekman transport driven by geostrophic wind stress is good to describe the intensity of coastal upwelling. Reasonable estimates of surface transport and coastal upwelling may be made using planetary boundary layer theory and the geostrophic wind approximation. Many publications refer to the Bakun (1973) technical memorandum that initially described the upwelling indices. In this method, Ekman mass transport is defined as the wind stress divided by the Coriolis parameter^[18]. Therefore, the increasing of high temporal and temporal resolution in wind product will be fed back into the improved understanding on quantitative intensity of coastal upwelling in the equatorial eastern Indian Ocean.

The rest of the paper is organized as follows. Section 2 describes in situ wind data and verifies the performance of CYGNSS observations. Section 3 describes the potential applications of this satellite measurement, including the MJO and the equatorial eastern Indian Ocean events. Section 4 provides a summary and discussion. Results from this study will advance our understanding of the quality and potential application of CYGNSS observations.

2 Validation of CYGNSS observations

In general, the results of recent verification studies of satellite winds come from the comparison between model simulations and satellite observations, or on the inter-comparison with in situ buoys^[19-20]. In this study, the performance of CYGNSS winds is compared with respect to in situ data, including observations from the Xisha Station and the Global Tropical Moored Buoy Array (GT MBA). Within this section, sea surface winds are examined over a 65-day period, from August 1 to October 4, 2017. This type of exercise gives a better understanding on the quality of CYGNSS wind in terms of these independent in situ observations. Part of this section describes the winds from Xisha flux tower and moored buoy winds in Indian, Pacific and Atlantic Ocean.

The Xisha flux tower is located in the South China Sea (SCS), which belongs to a mesoscale hydrological and marine meteorological observation network estab-

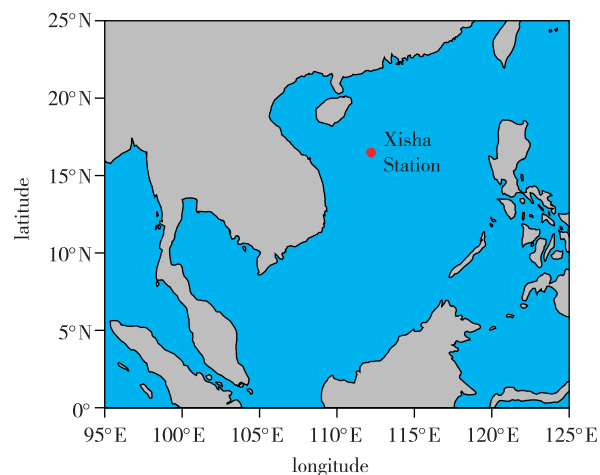


Fig. 2 Location of Xisha Station in South China Sea

lished by the SCS Institute of Oceanology. This flux tower is off the coast of Yongxing Island ($16^{\circ}49'N$, $112^{\circ}20'E$; see red point in Fig. 2 for its location), and categorized as both a coastal and a deep-sea station due to the deep water (more than 1 000 meters) basin of the northern-central SCS^[21-22]. This measurement provides meteorological parameters hourly, such as latent and sensible heat flux, carbon dioxide flux, and winds at a height of 5 m, 10 m, and 15m above the mean sea-level. Many efforts have also been made to verify the performance of observations from Xisha Station, such as the passages of tropical cyclones^[23], the response of heat flux to monsoon^[24], as well as the validation of satellite SST^[25].

In this study, moored buoy winds are also compared against CYGNSS observations. They are available from GT MBA through Pacific Marine Environmental Laboratory (www.pmel.noaa.gov). This moored buoy observing system is based on international cooperation and designed to provide real-time measurements for researching and forecasting tropical climate variations. It consists of three major components: the Research Moored Array for African-Asian-Australian Monsoon Analysis and Prediction (RAMA) in the Indian Ocean, the Tropical Atmosphere Ocean/Triangle Trans-Ocean Buoy Network (TAO/TRITON) in the Pacific and the Prediction and Research Moored Array in the Atlantic (PIRATA)^[26]. High quality time series data of these moored arrays have been advancing the research on air-sea interaction in time and space since their im-

plementations.

Note that only 7 buoys in RAMA, 47 buoys in TAO/TRITON and 7 buoys in PIRATA are considered in this study due to the time matching between in situ and satellite winds.Moored buoys are described in Table 1 and shown in Figure 3 (red points).Since satellite

winds over the sea surface are provided at the 10 meters neutral stability height, all moored buoy winds are adjusted from 3. 1–4. 0 meters to a height of 10 meters assuming neutral stability and using a logarithmic profile method^[25].This method requires only the wind speed at the reference height.

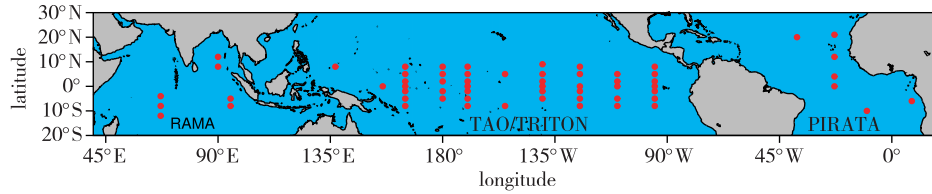


Fig. 3 Location of moored buoys from TAO/TRITON,PIRATA and RAMA arrays whose data are used in our comparison

Table 1 Statistical parameters of 61 moored buoys and CYGNSS wind speeds from August 1 to October 4,2017

Location	Mean buoy	Mean	RMSD/ (m/s)	Number of collocations	Location	Mean buoy	Mean	RMSD/ (m/s)	Number of collocations	
	wind speed/ (m/s)	CYGNSS wind speed/ (m/s)				wind speed/ (m/s)	CYGNSS wind speed/ (m/s)			
RAMA	67°E,4°S	7.44	6.77	2.38	73	140°W,2°N	8.28	7.08	2.26	69
	67°E,8°S	9.23	7.39	2.94	83	140°W,5°N	7.08	6.66	1.97	57
	67°E,12°S	9.92	7.77	3.21	91	140°W,9°N	6.80	6.99	2.09	52
	90°E,8°N	8.39	6.28	2.88	90	140°W,2°S	7.09	7.36	2.12	86
	90°E,12°N	8.20	6.35	2.91	80	140°W,5°S	8.41	7.66	2.13	90
	95°E,5°S	8.86	7.41	2.94	89	125°W,0°	6.68	5.88	1.85	78
	95°E,8°S	10.35	8.54	3.14	79	125°W,5°N	7.76	7.38	1.86	78
TAO/TRITON	137°E,8°N	5.37	4.49	2.00	42	125°W,8°N	7.39	7.51	2.27	71
	156°E,0°	5.67	4.93	1.78	66	125°W,2°S	6.61	5.95	1.75	80
	165°E,0°	6.54	6.28	1.78	52	125°W,5°S	8.92	7.67	2.59	77
	165°E,2°N	6.31	5.52	1.83	53	TAO/TRITON 125°W,8°S	8.58	7.74	2.23	75
	165°E,5°N	5.92	5.32	1.80	50	110°W,0°	5.80	5.47	1.63	47
	165°E,8°N	5.91	4.97	2.25	56	110°W,2°N	8.22	6.68	2.58	76
	165°E,2°S	6.07	5.46	1.94	42	110°W,5°N	7.62	7.77	2.31	81
	165°E,5°S	6.01	6.17	1.84	44	110°W,5°S	7.80	7.50	2.00	81
	165°E,8°S	7.39	7.98	2.26	83	110°W,8°S	9.08	8.54	2.37	79
	180°,2°N	7.02	6.86	3.13	84	95°W,0°	6.99	5.59	2.30	71
	180°,5°N	6.51	6.75	1.60	63	95°W,2°N	7.70	7.30	1.96	71
	180°,8°N	5.66	6.22	1.74	61	95°W,5°N	7.68	7.38	1.65	81
	180°,2°S	7.20	6.42	1.83	76	95°W,8°N	6.89	6.15	1.81	77
	180°,5°S	6.74	7.09	2.69	78	95°W,2°S	5.84	5.33	1.77	69
	170°W,0°	7.05	7.13	1.47	73	95°W,5°S	7.87	7.66	1.86	81
	170°W,2°N	7.44	6.97	1.76	42	95°W,8°S	9.21	8.39	2.12	73
	170°W,5°N	6.38	6.88	2.05	62	PIRATA	38°W,20°N	8.64	7.06	2.75
170°W,8°N	5.85	7.17	2.49	43	23°W,0°		7.22	6.88	1.93	87
170°W,2°S	7.79	7.43	1.87	81	23°W,4°N		7.79	7.28	2.08	79
170°W,5°S	6.86	7.58	2.07	78	23°W,12°N		6.69	5.85	2.40	66
170°W,8°S	7.41	7.90	2.76	87	23°W,21°N		7.84	6.64	2.45	124
155°W,5°N	6.71	6.88	1.70	79	10°W,10°S		9.00	8.20	2.68	84
155°W,8°S	8.08	8.20	2.09	72	8°E,6°S		5.50	4.53	1.59	76
140°W,0°	7.11	6.87	1.98	69						

Before deriving overall verification statistics, satellite winds are collocated with in situ winds only if they are spatially within a box of $0.2^\circ \times 0.2^\circ$ and temporally within 15 minutes. Each buoy wind is used only one time for collocation with the above mentioned resolutions. To make sure that the correct satellite wind is selected, the collocated pair is retained only if none of them conclude the missing data. Since science measurement requirements of CYGNSS mission is to provide wind speed over a dynamic range of 3–70 m/s as determined by a spatially averaged wind field with a resolution of 5.0×5.0 km, in situ winds below 3.0 m/s are not considered for collocation^[12].

Time series comparison of CYGNSS observations and in situ winds from Xisha flux tower is shown in Figure 4. The number of collocations of CYGNSS Level 2 version (L2) and Level 3 version (L3) data against in situ winds is 116 and 100. The L3 gridded wind product is surface wind speed, averaged in space and time (0.2° latitude and longitude, 1 hour). As shown in Figure 4a, CYGNSS L2 version data shows positive bias with respect to in situ wind from Xisha flux tower, while its time evolution is consistent with that of in situ winds. Figure 4b is similar to Figure 4a, but for L3 version. Reduced RMSD value (from 2.49 to 2.11) is obtained from the updated version of CYGNSS winds, suggesting a better performance of L3 version due to the gridding of irregular data.

The CYGNSS winds are also compared against buoy winds from RAMA, TAO/TRITON and PIRATA net works. Here, CYGNSS L3 data are used. A summary of comparison between CYGNSS and in situ observations is listed in Table 1. This table describes the mean buoy wind speed, the mean CYGNSS wind speed, their root-mean-square-difference (RMSD) and the number of collocations. Most of the CYGNSS wind speed values are lower than the buoy measured mean wind speeds. The quick revisit time of CYGNSS satellite on the same geographic points leads to larger number of collocations. The 65-day period is enough for the validation of CYGNSS observations. In addition, the mean RMSD is 2.17 m/s, which meets 2.0 m/s retrieval uncertainty for winds less than 20.0 m/s in terms of CYG-

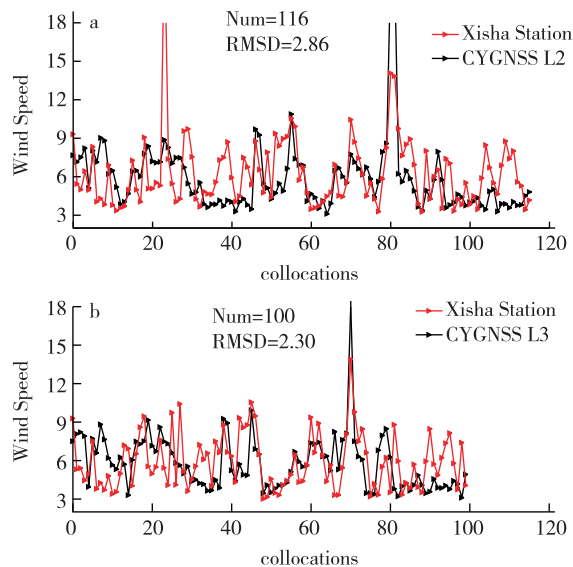


Fig. 4 Time series comparison of wind speeds between Xisha Station and (a) CYGNSS L2 and (b) L3 observations from August 1 to October 4 of 2017

NSS mission scientific data product baseline requirements. Part of this discrepancy may come from instrument error, and part of it may come from representative error because of not-exact match of in situ and satellite measurements. Although CYGNSS observations do well on the comparison against in situ winds, much work is needed to be done to increase the satellite data accuracy.

3 Applications

High-resolution, time-resolved sea surface wind datasets are needed to better understand, assess, and predict the complex mass and energy interchange processes of atmosphere and ocean, as well as to document any changes that occur because of long-term fluctuations, such as Madden-Julian oscillation (MJO) and coastal upwelling events. Global or tropical sampling for near-surface measurements is necessary to create the required datasets for these phenomena. Analyzing CYGNSS data from the perspective of eight tracks of specular points may enhance the accuracy and the spatio-temporal sampling of retrieved winds. In this section, we apply the results about the MJO and equatorial eastern Indian Ocean coastal upwelling events to discuss the potential applications of CYGNSS observations.

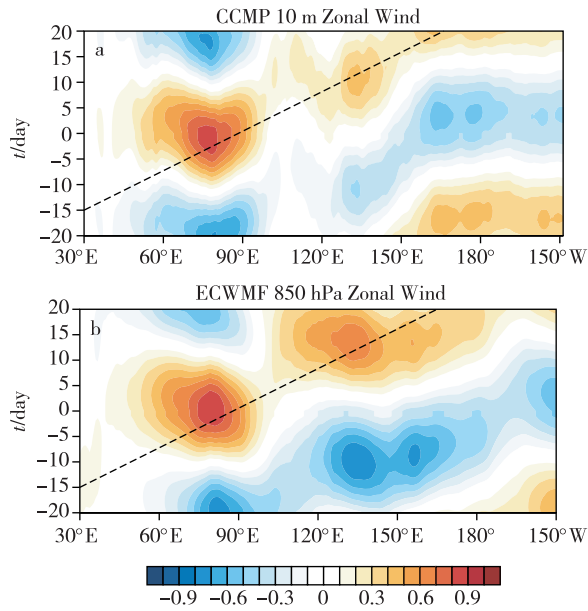


Fig. 5 (a) Longitude-time evolution of 30–60 day band-pass-filtered CCMP 10 m wind anomalies regressed against itself averaged over an eastern equatorial Indian Ocean box ($60^{\circ}\text{E}-90^{\circ}\text{E}, 5^{\circ}\text{S}-5^{\circ}\text{N}$) on a particular year (Regression coefficients are averaged over $10^{\circ}\text{S}-10^{\circ}\text{N}$; dashed lines in each panel denote the 5 m/s eastward propagation phase speed); (b) is similar to (a), but for 30–60 day band-pass-filtered ECMWF 850 hPa wind anomalies

One of the most distinctive signals of the Madden-Julian oscillation (MJO) is the upscale development and organization of convection in the Indian Ocean. To estimate the fidelity with respect to eastward propagation of MJO, 30–60 day filtered 850 hPa and 10 m zonal wind anomalies are regressed against the filtered wind anomalies averaged over an equatorial Indian Ocean box ($60^{\circ}\text{E}-90^{\circ}\text{E}, 5^{\circ}\text{S}-5^{\circ}\text{N}$), respectively, for time lags from day -20 to day $+20$. The lag-longitude sections of the regression coefficients are computed over longitudes $30^{\circ}\text{E}-150^{\circ}\text{W}$ by averaging the coefficients in the $10^{\circ}\text{S}-10^{\circ}\text{N}$ latitudinal band. The regression coefficient plots with respect to the reference box are shown in Figure 5. The maximum positive regression coefficients are located in the $60^{\circ}\text{E}-90^{\circ}\text{E}$ longitudinal band on day -5 to day $+5$. The eastward propagation phase speed of 5 m/s observed in wind fields is overlaid as a dashed line on all plots for comparison. The observed eastward propagating wind signals are reasonably detected by both 850 hPa and 10 m winds. Thus, 10

m wind can be used to detect the MJO signals, suggesting a potential application of CYGNSS observations.

To further show the potential applications of satellite winds in the eastern equatorial Indian Ocean, we compare the coastal upwelling indices against SST anomalies near the Java Island. The coastal upwelling indices are estimated from CCMP 10 m winds, and SST is available from Remote Sensing Systems Optimally Interpolated SST daily products at 25 km resolution. The time evolution of coastal upwelling indices shows remarkable agreement with that of SST anomalies from 2000 to 2011 (Fig. 6). When these indices decrease in the second half of the year, the SST anomalies also decrease. The standard deviations of upwelling indices and SST anomalies are 16.35 and 1.32. Such tight relationship between upwelling indices and SST variations suggests that the dynamical responses of SST in eastern equatorial Indian Ocean to atmospheric forcing exhibits a striking feature, with upwelling being associated with an enhanced offshore Ekman transport and wind speed. Sea surface wind is a good indicator to detect the intensity of coastal upwelling.

4 Conclusion

Near-surface winds over the ocean are major contributors to the momentum and energy fluxes at the air-sea interface. To understand the complex mass and energy interchange processes of atmosphere and ocean, high quality of sea surface wind product is key to properly modeling and forecasting the genesis and intensification of phenomena in the atmosphere and the ocean. The limitations of existing satellite measurements of sea surface winds under rainfall conditions become even more severe. By combining the all-weather performance of GPS-based bistatic scatterometry with the sampling properties of a dense satellite constellation, CYGNSS mission measures the ocean surface wind field with unprecedented temporal resolution and spatial coverage, under all precipitating conditions, and over the full dynamic range of wind speeds experienced in tropical cyclones. In short, the CYGNSS observation has the advantages as follows: 1. Little to no rainfall effect; 2. Quick

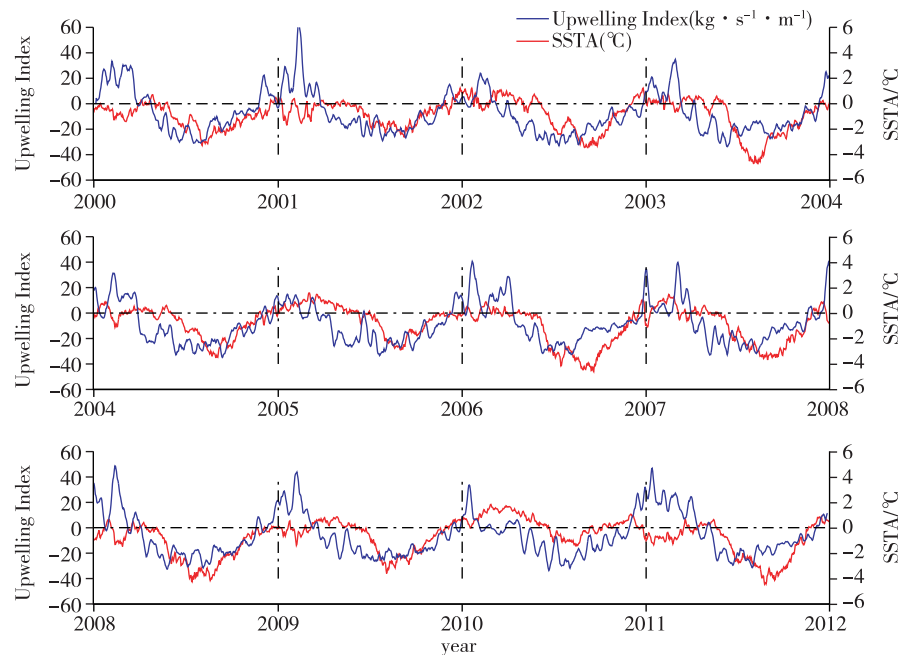


Fig. 6 Upwelling intensity around Java Island as detected by CCMP 10 m winds and SST anomalies

revisit time.

To verify the performance of satellite measurements, CYGNSS observations over the tropical areas between 35°N and 35°S are evaluated against in situ winds from Xisha flux tower in SCS and moored buoy winds from RAMA buoy network over the Indian Ocean, TAO/TRITON over the Pacific and PIRATA over the Atlantic during August – October 2017. Validation of CYGNSS winds shows maximum collocations in the Pacific Ocean due to the larger group of moored buoys in this area. The comparison of satellite and in situ winds are temporally and spatially separated within 15 minutes and 0.2° . CYGNSS winds show a mean RMSD of 2.17 m/s with respect to in situ winds, suggesting that wind speeds observed by CYGNSS agree with in situ winds.

CYGNSS observations have many potential applications, such as the detection of MJO and coastal upwelling signals. The version of CYGNSS winds updated with space-time homogeneity is better for studying the Indian Ocean and Western-Pacific Warm Pool. High quality and high temporal and spatial resolution sea surface wind data product from CYGNSS will advance the study of earth sciences.

References

- [1] Graham N E, Barnett T P. Sea surface temperature, surface wind divergence, and convection over tropical oceans [J]. *Science*, 1987, 238(4827) : 657-659
- [2] Smith S D. Coefficients for sea surface wind stress, heat flux, and wind profiles as a function of wind speed and temperature [J]. *J Geophys Res*, 1988, 93 (C12) : 15467-15472
- [3] Risien C M, Chelton D B. A global climatology of surface wind and wind stress fields from eight years of QuikSCAT scatterometer data [J]. *Journal of Physical Oceanography*, 2008, 38(11) : 2379-2413
- [4] Kumar B P, Vialard J, Lengaigne M, et al. TropFlux wind stresses over the tropical oceans: evaluation and comparison with other products [J]. *Climate Dynamics*, 2013, 40(7/8) : 2049-2071
- [5] Schlax M G, Chelton D B, Freilich M H. Sampling errors in wind fields constructed from single and tandem scatterometer datasets [J]. *Journal of Atmospheric and Oceanic Technology*, 2001, 18(6) : 1014-1036
- [6] Kalnay E, Kanamitsu M, Kistler R. The NCEP/NCAR 40-year reanalysis project [J]. *Bulletin of the American Meteorological Society*, 1996, 77(3) : 437-470
- [7] Kanamitsu M, Ebisuzaki W, Woolen J, et al. NCEP/DOE AMIP-II reanalysis (R-2) [J]. *Bulletin of the American Meteorological Society*, 2002, 83(11) : 1631-1643
- [8] Atlas R, Hoffman R N, Ardizzone J, et al. A cross-calibrated, multiplatform ocean surface wind velocity product for meteorological and oceanographic applications [J]. *Bulletin of the American Meteorological Society*, 2011, 92(2) : 157-174

- [9] Jones W L, Zec J. Evaluation of rain effects on NSCAT wind retrievals [C] // Oceans 96 MTS/IEEE, Prospects for the 21st Century, 1996: 1171-1176
- [10] Nie C, Long D G. The effect of rain on ERS scatterometer measurements [C] // IEEE International Conference on Geoscience and Remote Sensing Symposium, 2013: 4119-4121
- [11] Ruf C, Gleason S, Jelenak z, et al. The NASA EV-2 Cyclone Global Navigation Satellite System (CYGNSS) mission [C] // IEEE Aerospace Conference, 2013: 1-7
- [12] Ruf C S, Atlas R, Chang P S, et al. New ocean winds satellite mission to probe hurricanes and tropical convection [J]. Bulletin of the American Meteorological Society, 2012, 97(3): 150626133330005
- [13] Madden R A, Julian P R. Detection of a 40-50 day oscillation in the zonal wind in the tropical Pacific [J]. Journal of the Atmospheric Sciences, 1971, 28(5): 702-708
- [14] Wheeler M C, Hendon H H. An all-season real-time multivariate MJO index: development of an index for monitoring and prediction [J]. Monthly Weather Review, 2004, 132(8): 1917-1932
- [15] Demott C A, Klingaman N P, Woolnough S J. Atmosphere-ocean coupled processes in the Madden-Julian oscillation [J]. Reviews of Geophysics, 2015, 53(4): 1099-1154
- [16] Chen G X, Han W Q, Li Y L, et al. Intraseasonal variability of upwelling in the equatorial eastern Indian Ocean [J]. J Geophys Res, 2016, 120(11): 7598-7615
- [17] Schwing F B, O'Farrell M, Steger J M, et al. Coastal upwelling indices west coast of North America 1946-1995 [J]. Cambridge Studies in Applied Econometric, 1996, 47(1): 313
- [18] Bakun A. Coastal upwelling indices, west coast of North America, 1946-71 [R]. NOAA Technical Report NMFS SSRF-671, 1973: 103
- [19] Schulz E W, Kepert J D, Greenslade D J M. An assessment of marine surface winds from the Australian Bureau of Meteorology numerical weather prediction systems [J]. Weather & Forecasting, 2010, 22(3): 226-227
- [20] Rani S I, Gupta M D. Oceansat-2 and RAMA buoy winds: a comparison [J]. Journal of Earth System Science, 2013, 122(6): 1571-1582
- [21] Yang L, Wang D, Huang J, et al. Toward a mesoscale hydrological and marine meteorological observation network in the South China Sea [J]. Bulletin of the American Meteorological Society, 2015, 96(7): 150204133247008
- [22] Zeng L L, Wang Q, Xie Q, et al. Hydrographic field investigations in the northern South China Sea by open cruises during 2004-2013 [J]. Science Bulletin, 2015, 60(6): 607-615
- [23] Wang D X, Li J, Yang L, et al. The variations of atmospheric variables recorded at Xisha station in the South China Sea during tropical cyclone passages [M] // Hickey K. Advances in hurricane research-modelling, meteorology, preparedness and impacts. Rijeka, Croatia: InTech, 2012
- [24] Shi R, Guo X Y, Wang D X, et al. Seasonal variability in coastal fronts and its influence on sea surface wind in the northern South China Sea [J]. Deep-Sea Research Part II: Topical Studies in Oceanography, 2015, 119: 30-39
- [25] Qin H L, Chen G X, Wang W Q, et al. Validation and application of MODIS-derived SST in the South China Sea [J]. International Journal of Remote Sensing, 2014, 35(11/12): 4315-4328
- [26] McPhaden M J. The global tropical moored buoy array [C] // Proceedings of OceanObs'09 Sustained Ocean Observations & Information for Society, 2010, DOI: 10.5270/OceanObs09.cwp.61